

Ligand Binding and Thermostability of Different Allosteric States of the Insulin Zinc–Hexamer

Kasper Huus,*[‡] Svend Havelund,[§] Helle B. Olsen,[§] Bent W. Sigurskjold,^{||} Marco van de Weert,[‡] and Sven Frokjaer[‡]

Department of Pharmaceutics and Analytical Chemistry, The Danish University of Pharmaceutical Sciences, Universitetsparken 2, 2100 Copenhagen, Denmark, Diabetes Protein Engineering, Novo Nordisk A/S, Novo Allé 1, 2880 Bagsværd, Denmark, and Institute of Molecular Biology and Physiology, University of Copenhagen, Universitetsparken 13, 2100 Copenhagen, Denmark

Received December 1, 2005; Revised Manuscript Received February 7, 2006

ABSTRACT: The influence of ligand binding and conformation state on the thermostability of hexameric zinc–insulin was studied by differential scanning calorimetry (DSC). The insulin hexamer exists in equilibrium between the forms T₆, T₃R₃, and R₆. Phenolic ligands induce and stabilize the T₃R₃- and R₆-states which are further stabilized by binding of certain anions that do not stabilize the T₆-state. It was shown that the thermostability of the resorcinol-stabilized R₆-state was significantly higher than that of the T₆-state. Further analysis showed that phenol- and *m*-cresol-stabilized R₆-hexamer loses three ligands before reaching the unfolding temperature and hence unfolds from the T₃R₃-state. The relative affinity of the four tested anionic ligands was found, by DSC, to be thiocyanate ≥ 4-hydroxy-3-nitrobenzoate >> *p*-aminobenzoate >> chloride. The results correlate with other methods and demonstrate that DSC provides a general and useful method of evaluation of both phenolic and anionic ligand binding to insulin without the use of probes or other alterations of the system of interest. However, it is a prerequisite that the binding is strong enough to saturate the binding sites at temperatures around the unfolding transition.

The interaction between proteins and ligands is fundamental in countless biological systems. The majority of protein–ligand complexes involve noncovalent interactions, and the binding affinity is determined by both enthalpic and entropic factors. Formation of a complex between a ligand and native protein usually results in an increased thermodynamic stability of the protein, and often, the interaction leads to conformational changes in the protein. The objective of the present study is to evaluate the effects of ligand binding and protein conformation on the thermostability of recombinant human insulin.

At the low concentration found in the bloodstream, insulin exists as a monomer, which is the biologically active form. At higher concentrations, insulin assembles to dimers and, in the presence of zinc ions at neutral pH, to hexamers. Following biosynthesis, insulin is stored as crystalline zinc-bound hexamers in vesicles within the pancreatic β -cells from which secretion occurs in response to elevated blood glucose levels (1). Centrally located in the insulin hexamer are six His^{B10} residues which bind two zinc ions. In insulin crystals, up to 10 additional zinc ions have been found in other sites. However, it is not clear to what extent these additional sites are also present in insulin hexamers in solution (2–5). The hexamer is known to exist in three different conformations which have been given the nomenclature T₆, T₃R₃, and R₆, depending on the conformations of the monomer subunits. The principal difference is that the residues B1–B8 are

converted from an extended conformation in the T-state to an α -helix in the R-state. Ligand binding to allosteric sites on the hexamer is required to change the conformation from T- to R-state (6). The transformation creates hydrophobic pockets in which phenol and phenol derivatives have been shown to bind. There are three phenolic pockets in the T₃R₃ and six in the R₆ hexamer. Furthermore, the conformation change causes each of the two zinc ions to adopt a coordination comprising three B10 histidines and one small-molecule monovalent anionic ligand (6, 7). The role of ligand binding and the allosteric properties of the insulin hexamer have recently been reviewed (8). It is still not known in which allosteric state insulin is stored in the pancreatic β -cells, and the identities of any in vivo allosteric ligands are not known, but believed to exist (8).

Phenolic compounds (phenol, *m*-cresol, and methylparaben) have been used as antimicrobial preservatives in insulin formulations long before the specific phenolic pockets in the hexamer became known (9). The hexamer-stabilizing effect of the phenolic preservatives is reflected in their ability to improve the chemical stability of insulin formulations. Thus, phenolic preservatives have been found to reduce the rate of formation of deamidation products and covalent di- and polymers in insulin formulations (10). The improved chemical stability presumably correlates with the affinity of the preservative to the phenolic pocket in the insulin hexamer.

Several examples of more direct methods of determining the binding of phenolic ligands to the insulin hexamer are described in the literature. The spectroscopic feature of Co²⁺–insulin has been used to study the ability of different ligands in driving the T₆ to R₆ transition (11, 12). Another approach exploits spectral changes caused by the extraction

* To whom correspondence should be addressed. E-mail, kaan@funi.dk; phone, +45 3530 6236; fax, +45 3530 6030.

[‡] The Danish University of Pharmaceutical Sciences.

[§] Novo Nordisk A/S.

^{||} University of Copenhagen.

of Zn^{2+} or Co^{2+} from the insulin hexamer by complexing agents (6, 13–16). The hexamer-stabilizing effect of phenol and resorcinol have been investigated using 2,2',2''-terpyridine, which can also be used to differentiate the hexamer-stabilizing effect of anionic ligands (17). Yet another approach has been to use chromophoric anionic ligands to the His^{B10}-zinc-site as probes for the T₆ to R₆ transition. The surroundings of the probes change upon the T to R transformation, and this changes the spectroscopic features of the probes. One example of such probes is 4-hydroxy-3-nitrobenzoate (4H3N).¹ The absorbance and circular dichroism spectra of 4H3N are significantly changed when it is bound at R-state His^{B10} sites of the insulin hexamer. The probe has been used in evaluation of ligands to the phenolic pockets (18) and in displacement studies with non-chromophoric anionic ligands to the His^{B10} sites of both Zn^{2+} and Co^{2+} R₆ hexamers (19). Another example of His^{B10}-zinc-site anionic binding chromophoric probes is 2-(1-(2-hydroxy-5-sulfophenyl)-3-phenyl-5-formazano)benzoic acid (20). Recently, ¹⁹F NMR has been applied to evaluate the binding affinities of trifluoromethyl-substituted aromatic carboxylates to the anionic binding sites in Zn^{2+} and Co^{2+} insulin hexamers (21).

Isothermal titration calorimetry (ITC) has been applied to determine the binding thermodynamics of phenolic ligands to the insulin hexamer (22–24). Determination of binding affinities of the phenolic ligands is complicated by the cooperativity of the system, and fitting of the ITC data required a complex hierarchical series of models involving some simplifications and assumptions. (22). However, one major advantage of calorimetric methods is that they are general and no interfering probes are needed, so the system can be studied directly without modifications.

It is the objective of the present work to examine the influence of ligand binding and hexamer conformation on the thermostability of native human insulin. Differential scanning calorimetry (DSC) will be applied to examine whether stabilization of the T₃R₃ and R₆ zinc–insulin hexamer conformation is reflected in increased thermostability of the hexamer compared to the T₆ conformation. It has previously been shown that both phenolic and anionic ligand affinity to the R₆ hexamer is correlated to the stability of hexamers as measured by 2,2',2''-terpyridine removal of Zn^{2+} (17). It will be examined whether the ligand affinities are correlated to the thermostability and whether DSC can provide a useful method of determining relative binding affinities of both phenolic and anionic ligands. Preferential ligand binding to the native state of a protein manifests itself in increases in the T_m of protein denaturation, whereas preferential binding to the unfolded state decreases the T_m . The change in T_m is proportional to the association constant and concentration of the ligand binding to the native or unfolded protein. In the case where a ligand binds to both the native and unfolded protein, the change in T_m is proportional to the difference between the affinities (25). We hypothesize that changes in T_m of insulin hexamer thermal denaturation can be used as a measure of the relative affinities

of the phenolic and anionic ligands. Ligands which have been evaluated by other methods will be examined, and these include the phenolic ligands phenol, *m*-cresol, and resorcinol and the anionic ligands chloride (NaCl), thiocyanate (KSCN), *para*-aminobenzoate (PABA), and 4-hydroxy-3-nitrobenzoate (4H3N). In the presence of His^{B10}-anionic ligands, it has been shown that resorcinol, phenol, and *m*-cresol apparently shift the allosteric equilibrium in favor of the R₆-state. However, in the absence of anionic ligands, it appears that the *m*-cresol-induced transition is incomplete and both R- and T-states are stabilized in the Co(II)-hexamer (12). Apparently, no studies examining the difference between phenol and *m*-cresol binding in the absence or presence of anionic ligands have been conducted with Zn–insulin. Therefore, in the present work, 4H3N will be applied as a spectroscopic probe (18, 19) in low and high concentration in experiments with resorcinol, phenol, and *m*-cresol.

MATERIALS AND METHODS

Materials. Zinc-free native human insulin was obtained from Novo Nordisk A/S. All other chemicals were commercially available chemicals of analytical grade. Deionized water was filtered using a Millipore system (Millipore, Billerica, MA) and used for all samples. All insulin samples were made from fresh stock solutions, and the concentrations were determined from the absorbance at 276 nm using $\epsilon_{276} = 6200 \text{ M}^{-1} \text{ cm}^{-1}$ (26).

UV–Vis Absorption Binding Isotherms. The His^{B10}-zinc-site anionic ligand 4-hydroxy-3-nitrobenzoic acid (4H3N) was used as a chromophoric probe in UV–vis absorption binding curves for phenol, *m*-cresol, and resorcinol. The method was performed as previously described by Bloom et al. (18) but in the absence of *p*-amino benzoic acid (PABA). Samples were prepared in 7 mM phosphate buffer at pH 7.4 using a high ratio of 4H3N (0.6 mM insulin with 0.225 mM 4H3N) and a low ratio of 4H3N (2.0 mM insulin with 0.15 mM 4H3N). UV–vis absorbance spectra were collected on a Cary 300 Bio UV–Vis Spectrophotometer (Varian, Palo Alto, CA). The apparent dissociation constants, K_D , were obtained by fitting the binding isotherms to the hyperbolic equation $\text{Abs} = [\text{L}]/([\text{L}] + K_D)$ where [L] is the ligand concentration.

Differential Scanning Calorimetry (DSC). Data collection was performed using a VP-DSC differential scanning calorimeter (MicroCal, LLC, Northampton, MA) (27). Temperature scans were performed from 25 to 110 °C at a scan rate of 1 °C/min and an excess pressure of 0.21 MPa with 7 mM phosphate buffer in the reference cell. All insulin samples were prepared in 7 mM phosphate buffer adjusted to pH 7.4 with perchloric acid and/or sodium hydroxide. The samples and references were degassed immediately before use. A buffer–buffer reference scan was subtracted from each sample scan prior to concentration normalization. Baselines were created in Origin 7.0 (OriginLab, Northampton, MA) by cubic interpolation of the pre- and post-transition baselines. Subsequent calculations of thermodynamic parameters were performed in a spreadsheet. The calorimetric enthalpy is given by the following equation:

$$\Delta H_{\text{cal}} = \int_{T_0}^T C_p \, dT \quad (1)$$

¹ Abbreviations: DSC, differential scanning calorimetry; PABA, *para*-aminobenzoic acid; 4H3N, 4-hydroxy-3-nitrobenzoic acid; ΔH_{cal} , calorimetric enthalpy, ΔH_{vH} , van't Hoff enthalpy; C_p , excess heat capacity; T_m , transition midpoint; T_{max} , temperature of maximum C_p .

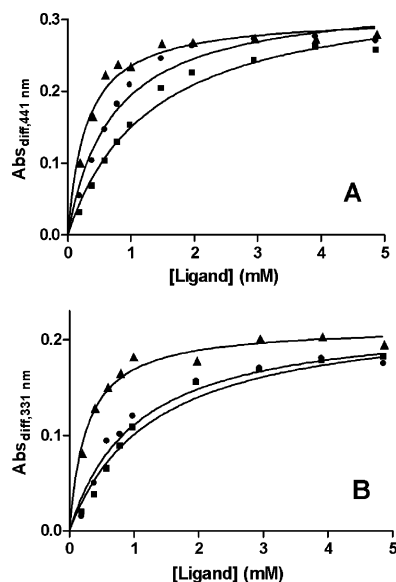


FIGURE 1: Titration of zinc-insulin with phenolic ligands *m*-cresol (squares), phenol (circles), and resorcinol (triangles). (A) 2.0 mM insulin (2 Zn²⁺/hexamer) and 0.15 mM 4H3N; (B) 0.6 mM insulin (2 Zn²⁺/hexamer) and 0.225 mM 4H3N. The absorbance at 446 nm, calculated by subtracting the spectra of the ligand-free samples from the spectra of the ligand-bound samples, is plotted as a function of ligand concentration.

Table 1: Dissociation Constants of the Phenolic Ligand-Induced Insulin T to R Transition^a

ligand	2.0 mM insulin, 0.15 mM 4H3N K_D (mM)	0.6 mM insulin, 0.225 mM 4H3N K_D (mM)
<i>m</i> -Cresol	1.31 ± 0.19	1.28 ± 0.24
Phenol	0.76 ± 0.09	1.02 ± 0.20
Resorcinol	0.30 ± 0.04	0.27 ± 0.04

^a The values are from the absorption binding curves of the phenolic ligand titrations in the presence of the chromophoric probe 4H3N (Figure 1).

where C_p is the excess heat capacity. Accordingly, ΔH_{cal} is calculated as the area under the baseline-corrected C_p -curve obtained for each sample. The transition midpoint, T_m , is defined as the temperature at which the transition is half-completed, that is, when half of the area under the C_p -curve is on either side of T_m . T_{max} is the temperature at which C_p is at its maximum ($C_{p,max}$).

RESULTS

Spectroscopic Titrations with Phenolic Ligands. 4H3N was used as a probe for the T to R transition induced by phenolic ligands (phenol, *m*-cresol, and resorcinol). Two titrations with each phenolic ligand were performed; one with a low, and one with a high ratio of 4H3N relative to the number of His^{B10}-zinc-sites. Low and high saturation of the anionic binding sites was used to examine the relative effect of anionic binding on the binding of the phenolic ligands. The low ratio (panel A in Figure 1) was 0.225 molecules of 4H3N per binding site. The high ratio (panel B in Figure 1) was 1.125 molecules of 4H3N per binding site. Values of dissociation constants, K_D , of the phenolic binding are given in Table 1. With both ratios of 4H3N, resorcinol is clearly a stronger ligand than phenol and *m*-cresol. At the high ratio

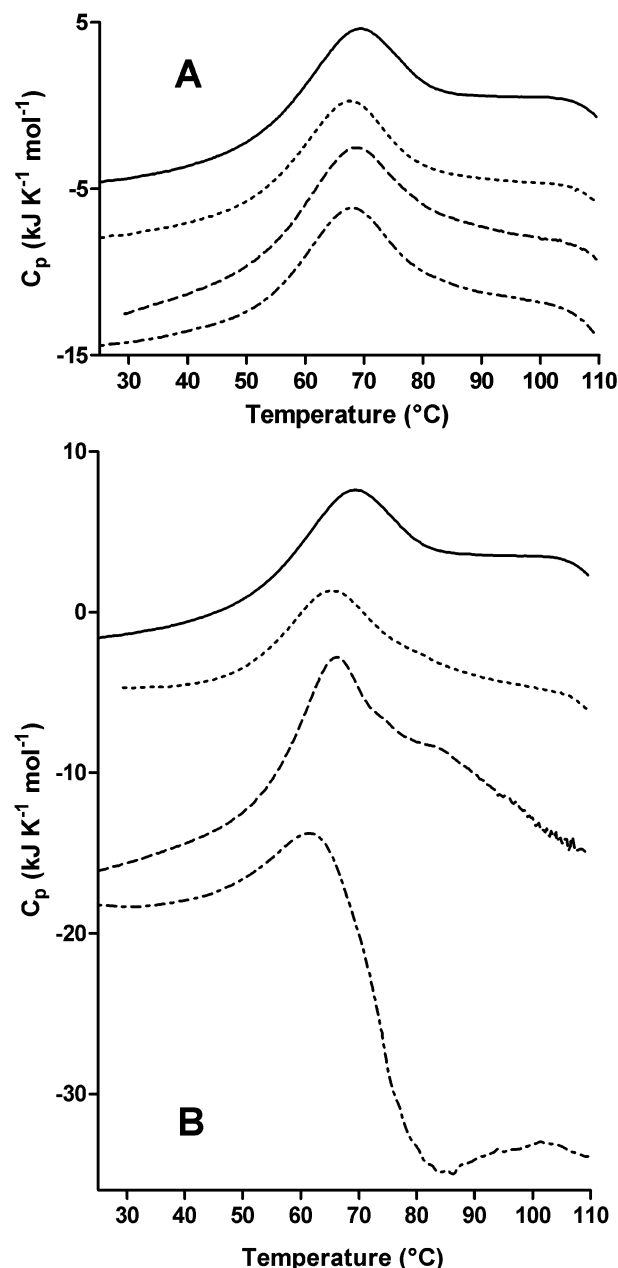


FIGURE 2: DSC thermograms of 0.6 mM human insulin, zinc-free, in 7 mM phosphate buffer at pH 7.4. Full line, no ligand; dotted line, phenol; dashed line, resorcinol, and dashed-dotted line, *m*-cresol. Panel A shows samples with 20 mM ligand compared to a ligand-free sample. Panel B shows the samples with 100 mM ligand compared to a ligand-free sample. All scans are shown without baseline correction.

of 4H3N, the binding of phenol and *m*-cresol is practically identical, but at the low 4H3N ratio, *m*-cresol is significantly weaker than phenol and it reaches a lower level of absorbance.

DSC Results with Phenolic Ligands. The effect on the thermostability obtained by addition of phenolic ligands to zinc-free and zinc-bound native human insulin is shown in Figures 2 and 3, and T_{max} values are compiled in Table 2. At the concentration used here, zinc-free human insulin at neutral pH does not form thermostable hexamers and is primarily dimeric, which means that the phenolic binding pocket is not present. At 20 mM, all three phenolic ligands have a slight and comparable destabilizing effect on zinc-

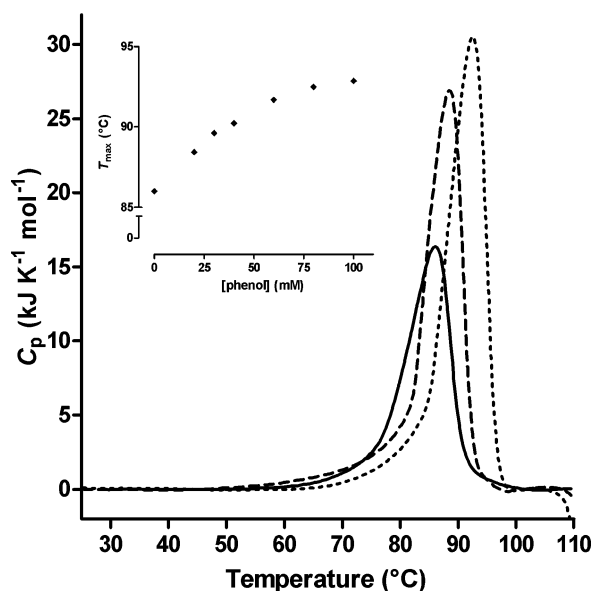


FIGURE 3: DSC thermograms of 0.6 mM human insulin, 0.5 mM Zn^{2+} , in 7 mM phosphate buffer at pH 7.4. Full line, 0 mM phenol; dashed line, 20 mM phenol; and dotted line, 80 mM phenol. For clarity, only two phenol concentrations are shown in the graph. The inset shows all T_{max} values plotted as a function of phenol concentration.

Table 2: Effects of Phenolic Ligands on 0.6 mM Zinc-Free Insulin at pH 7.4 in 7 mM Phosphate Buffer^a

ligand	T_{max} (°C)
No ligand ($n = 3$) \pm SD	68.7 \pm 0.3
20 mM phenol	67.8
20 mM resorcinol	67.8
20 mM <i>m</i> -cresol	67.5
100 mM phenol	65.0
100 mM resorcinol	65.6
100 mM <i>m</i> -cresol	61.4

^a The shown results are the T_{max} values from DSC experiments.

free insulin expressed by small decreases in T_{max} (see Figure 2A and Table 2). The decrease in T_{max} was 0.9, 0.9, and 1.2 °C for 20 mM phenol, resorcinol, and *m*-cresol, respectively. In the presence of 100 mM ligand, there was a pronounced difference between the ligands. The decrease in T_{max} compared to a ligand-free sample was 3.7 and 3.1 °C in the presence of 100 mM phenol and resorcinol, respectively. In the presence of 100 mM *m*-cresol, T_{max} was reduced by 7.3 °C, which is significantly more than observed with 100 mM phenol or resorcinol. As shown in Figure 2A, 20 mM of the three phenolic ligands did not alter the appearance of the DSC thermogram; they only decreased the T_{max} slightly. At 100 mM ligand concentration, the thermograms are slightly altered by phenol and resorcinol and significantly altered by *m*-cresol (Figure 2B). With 100 mM *m*-cresol, an exothermic transition immediately follows, and probably to some extent overlaps with, the unfolding endotherm.

We have previously shown that the thermostability of human insulin is strongly correlated to its association state (28). Hexameric zinc-insulin dissociated and unfolded with a thermal midpoint of transition (T_m) approximately 20 °C higher than the T_m of dissociation and unfolding of dimeric zinc-free insulin. At zinc concentrations below 5 Zn^{2+} per insulin hexamer, a biphasic thermal denaturation profile with both a dimer and a hexamer denaturation transition was

observed (28). Therefore, in the present study, a high zinc concentration (5 Zn^{2+} per insulin hexamer) is used to ensure that the system only exhibits one transition, the concurrent dissociation and unfolding of the insulin hexamer.

Contrary to the destabilizing effect observed on zinc-free insulin, zinc-insulin exhibits a significant increase in thermostability in the presence of phenolic ligands. The remarkable effect of 20 and 80 mM phenol on the thermostability of human insulin containing 5 Zn^{2+} /hexamer in the absence of anionic ligands is shown in Figure 3. The increase in T_{max} compared to a phenol-free sample is 2.4 and 4.7 °C, respectively. Similarly, the increase in T_{max} in samples containing 20 mM *m*-cresol and resorcinol in the absence of anionic ligands was 2.5 and 3.3 °C, respectively. A series of experiments by DSC were performed with various concentrations of phenolic ligands and constant protein concentration in the absence of anionic ligand and in the presence of 50 mM NaCl. The T_{max} as a function of phenol concentration in the absence of anionic ligand is plotted in the inset in Figure 3. The stabilizing effect of the phenolic ligands all caused a rise in T_{max} apparently approaching a maximum value, but only *m*-cresol reached a plateau both in the absence and presence of the anionic ligand NaCl. As can be seen by the area under the transition curves in Figure 3 and the values in Table 3, the calorimetric enthalpy of denaturation (ΔH_{cal}) increases significantly in the presence of phenolic ligands. In the absence of anionic ligand, ΔH_{cal} is 250 and 252 kJ/mol for phenol and *m*-cresol, respectively, compared to 173 kJ/mol when no phenolic ligand is present. In the presence of resorcinol, ΔH_{cal} further increases to 286 kJ/mol. In the presence of 50 mM NaCl, the values of ΔH_{cal} were 260, 267, and 287 kJ/mol for *m*-cresol, phenol, and resorcinol, respectively. The increases in T_{max} were higher in the presence of NaCl, and again resorcinol gave the largest increase in T_{max} . Analogous to the experiments in the absence of anionic ligands, phenol and *m*-cresol gave similar increases in T_{max} (until a plateau was reached at high *m*-cresol concentrations).

We have previously shown that hexameric insulin undergoes essentially reversible two-state unfolding with simultaneous protein dissociation during thermal denaturation (28). The reversibility after reheating a sample that had previously been heated to near-completion of the transition was approximately 80%. Also, it was shown that scan rate variation had just a minor effect on the T_{max} , indicating that the process is not predominantly kinetically controlled (28). Assuming that ligand-bound insulin hexamer undergoes reversible two-state unfolding with simultaneous dissociation and ligand loss



where N is the native protein, L is a ligand, and U is the unfolded protein, then the effect of ligand concentration on T_{max} at constant protein concentration is given by the following equation (29):

$$\ln[L] = \frac{-\Delta H_{vH,s}}{mRT_{\text{max}}} + A \quad (3)$$

where $\Delta H_{vH,s}$ is the van't Hoff enthalpy, R is the gas constant, and A is a constant. Plots of $\ln[L]$ versus $1/T_{\text{max}}$ have a slope of $-\Delta H_{vH,s}/mR$. The number of ligand binding sites, m , can

Table 3: Thermodynamic Parameters Obtained from Analysis of the DSC Experiments with Phenolic Ligands and Zinc–Insulin in the Absence and Presence of 50 mM NaCl^a

ligand	ΔH_{cal} (kJ/mol) ^b	$\Delta H_{\text{vH,cal}}$ (kJ/mol) ^c	$\Delta H_{\text{vH,cal}}/\Delta H_{\text{cal}}$	$\Delta H_{\text{vH,s}}$ (kJ/mol) ^d	Goodness of fit (r^2) ^d	$K_{\text{D},90^\circ\text{C}}$ (mM) ^e
No ligand	173 ± 3	1218 ± 9	7.1 ± 0.1	-	-	-
50 mM NaCl	179	1266	7.1	-	-	-
<i>m</i> -Cresol	250 ± 7	1457 ± 26	5.8 ± 0.2	200 ± 24	0.968	25
Phenol	252 ± 6	1485 ± 52	5.9 ± 0.1	186 ± 7	0.996	23
Resorcinol	286 ± 15	1615 ± 151	5.6 ± 0.3	204 ± 9	0.995	15
<i>m</i> -Cresol + 50 mM NaCl	260 ± 7	1642 ± 53	6.3 ± 0.3	171 ± 8	0.994	4.7
Phenol + 50 mM NaCl	267 ± 6	1638 ± 56	6.1 ± 0.2	179 ± 12	0.977	4.6
Resorcinol + 50 mM NaCl	287 ± 6	2001 ± 179	7.0 ± 0.8	201 ± 3	0.999	4.3

^a The enthalpies are the average of the results performed with varying concentrations of each ligand. The enthalpies are given per monomer of insulin ± standard deviation. ^b Area under the curve of the individual excess heat capacity curve. ^c Calculated by eq 7. ^d Best linear least-squares fit of the $\ln[L]$ versus $1/T_{\text{max}}$ data according to eq 3 assuming 6 binding sites per insulin hexamer for resorcinol and 3 binding sites for phenol and *m*-cresol. ^e Calculated according to eqs 5 and 6. Values are estimated to be in error by no more than 10%.

Table 4: Number of Ligand Binding Sites Per Insulin Hexamer As Determined by Fitting of the DSC Data to eq 4

phenolic ligand	without Cl ⁻	50 mM Cl ⁻
Phenol	2.94 ± 0.12	3.30 ± 0.30
<i>m</i> -Cresol	2.52 ± 0.24	2.70 ± 0.30
Resorcinol	5.46 ± 0.24	5.76 ± 0.12
anionic ligand	40 mM phenol	40 mM resorcinol
NaCl	0.51 ± 0.07	-
PABA	0.64 ± 0.07	-
4H3N	1.14 ± 0.14	-
KSCN	1.12 ± 0.06	1.88 ± 0.10

be estimated by fitting data to the following equation (29):

$$\frac{(\Delta H_0 - \Delta C_{p0} T_{\text{max}0})}{RT_{\text{max}}} - \frac{\Delta C_{p0} \ln(T_{\text{max}}/T_{\text{max}0})}{R} + m \ln[L] = B \quad (4)$$

where ΔH_0 , ΔC_{p0} , and $T_{\text{max}0}$ are the denaturation enthalpy, heat capacity change, and T_{max} of the ligand-free protein. To apply these equations, it is required that the ligand concentration is much larger than the concentration of binding sites on the protein (29). The results of fitting to the DSC results of the phenolic ligands to eq 4 are shown in Table 4. The numbers of binding sites per insulin hexamer were close to 3 for phenol and *m*-cresol and close to 6 for resorcinol, both in the absence and presence of NaCl. Plots of $\ln[L]$ as a function of $1/T_{\text{max}}$ (van't Hoff plots according to eq 3) of phenol, resorcinol, and *m*-cresol are shown in Figure 4. The lowest concentration of the phenolic ligands used in the van't Hoff analysis was 20 mM, and the concentration of putative binding sites for the ligands was held constant at 0.6 mM. Results of the van't Hoff analysis are given in Table 3, and they are based on the number of binding sites obtained by eq 4 (see Table 4). There are only slight differences in the values of $\Delta H_{\text{vH,s}}$ obtained with the different ligands. The T_{max} of the zinc–insulin thermal denaturation with *m*-cresol reached a plateau above 50 mM *m*-cresol, and therefore, these points were omitted from the van't Hoff analysis both in the absence and presence of NaCl. A probable explanation of the plateau for *m*-cresol is given in the discussion.

The dissociation constant of the ligand–protein complex is proportional to the increase in T_m of the ligand-bound protein ($T_{m,L}$) compared to the T_m of ligand-free protein ($T_{m,0}$). The apparent dissociation constant at the denaturation

temperature, $K_{\text{D}(T_m,L)}$, is given by the following equation (25, 30):

$$T_{m,L} - T_{m,0} = \frac{mT_{m,L}T_{m,0}R}{n\Delta H_{\text{cal},0}} \ln(1 + [L]K_{\text{D}(T_m,L)}) \quad (5)$$

where $\Delta H_{\text{cal},0}$ is the calorimetric enthalpy of the ligand-free protein. Following the calculation of $K_{\text{D}(T_m,L)}$, an apparent dissociation constant at a reference temperature can be calculated by the van't Hoff expression

$$\frac{d \ln K_D}{d(1/T)} = - \frac{\Delta H_{\text{vH,s}}}{R} \quad (6)$$

The dissociation constants were calculated at 90.0 °C where linearity was observed in the van't Hoff plots with the T_m values of all three ligands (data not shown). Again, it was assumed that for phenol and *m*-cresol 3 molecules bind per hexamer and that for resorcinol 6 molecules bind per hexamer. In the absence of anionic ligand, the resulting apparent dissociation constants, $K_{\text{D},90^\circ\text{C}}$ were 15, 23, and 25 mM for resorcinol, phenol, and *m*-cresol, respectively. In the presence of 50 mM NaCl, the apparent dissociation constants were 4.3, 4.6, and 4.7 mM for resorcinol, phenol, and *m*-cresol, respectively. Calculation of the dissociation constant by eq 5 assumes that the ligand only binds to the folded state of the protein. The destabilization found by the phenolic ligands on zinc-free insulin indicates some degree of binding to the unfolded state which will be similar in the case of unfolded zinc–insulin. Consequently, the dissociation constants may be slightly underestimated and are therefore referred to as apparent dissociation constants.

The calorimetric van't Hoff enthalpy is derived from the van't Hoff expression, and for oligomeric proteins with n subunits, it can be calculated by the following equation (31, 32):

$$\Delta H_{\text{vH,cal}} = (\sqrt{n} + 1)^2 RT_m^2 \frac{C_{p,\text{max}}}{\Delta H_{\text{cal}}} \quad (7)$$

where $C_{p,\text{max}}$ is the maximum excess heat capacity. As follows from eq 7, the calorimetric van't Hoff enthalpy is dependent on the shape of the denaturation transition peak. The ratio $\Delta H_{\text{vH,cal}}/\Delta H_{\text{cal}}$ is a measure of the validity of the assumed two-state transition. Ratios lower than unity are indicative of intermediate states, and ratios above unity are

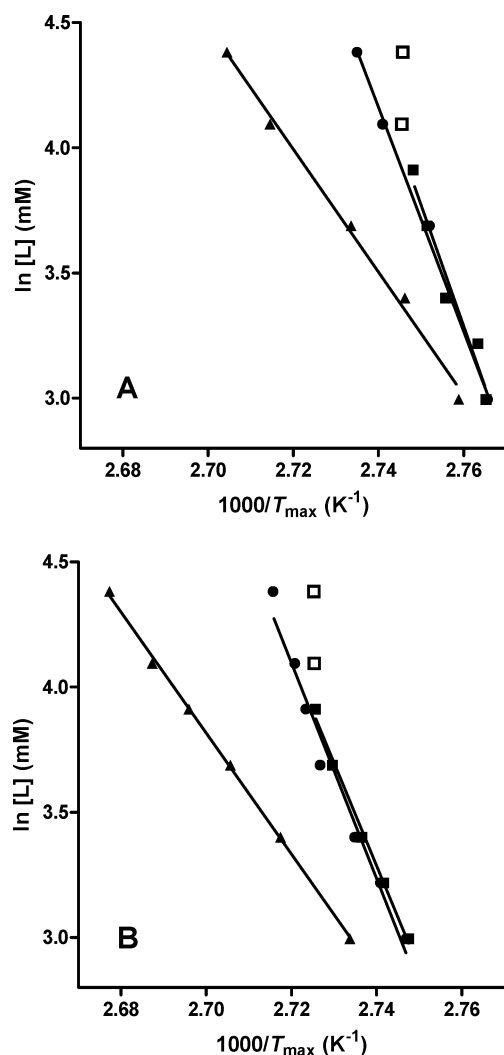


FIGURE 4: van't Hoff plot according to eq 3. The logarithms of the ligand concentrations (mM) are plotted as a function of $1/T_{\max}$ (K^{-1}). Samples contained 0.6 mM human insulin, 0.5 mM Zn^{2+} , and 7 mM phosphate at pH 7.4 and (A) absence of anionic ligand; (B) presence of 50 mM NaCl. Ligand legends: *m*-cresol (filled and open squares), phenol (filled circles), and resorcinol (filled triangles). The straight lines are the best fit of the data to eq 3. The *m*-cresol data points shown as open squares are excluded from the linear fit (explanation is given in Discussion).

interpreted as cooperative unfolding of oligomers (31). Values of $\Delta H_{\text{vH,cal}}$ have been calculated for each phenolic ligand and are shown in Table 3 with the $\Delta H_{\text{vH,cal}}/\Delta H_{\text{cal}}$ ratios. The ratio was close to 7 for hexameric zinc-insulin in the absence of ligands (i.e., in the T_6 -state). In the presence of phenolic ligands, the ratios were close to 6 but higher (7 ± 0.8) with resorcinol in the presence of 50 NaCl. We note that the two different van't Hoff enthalpies reported here cannot be compared. A van't Hoff enthalpy is always based on a model. The van't Hoff enthalpy calculated according to eq 7 ($\Delta H_{\text{vH,cal}}$) relates to the denaturation (dissociation and unfolding) of the protein and does not directly involve ligand interaction except for the effect that ligands possibly might have on the shape of the transition peaks. The van't Hoff enthalpies ($\Delta H_{\text{vH,s}}$) calculated from the slopes of the $\ln[L]$ versus $1/T_{\max}$ relate to the ligand binding and are a measure of the temperature dependency of the affinity (25).

DSC Results with Anionic Ligands. The effect of the anionic ligands NaCl, KSCN, PABA, and 4H3N on the

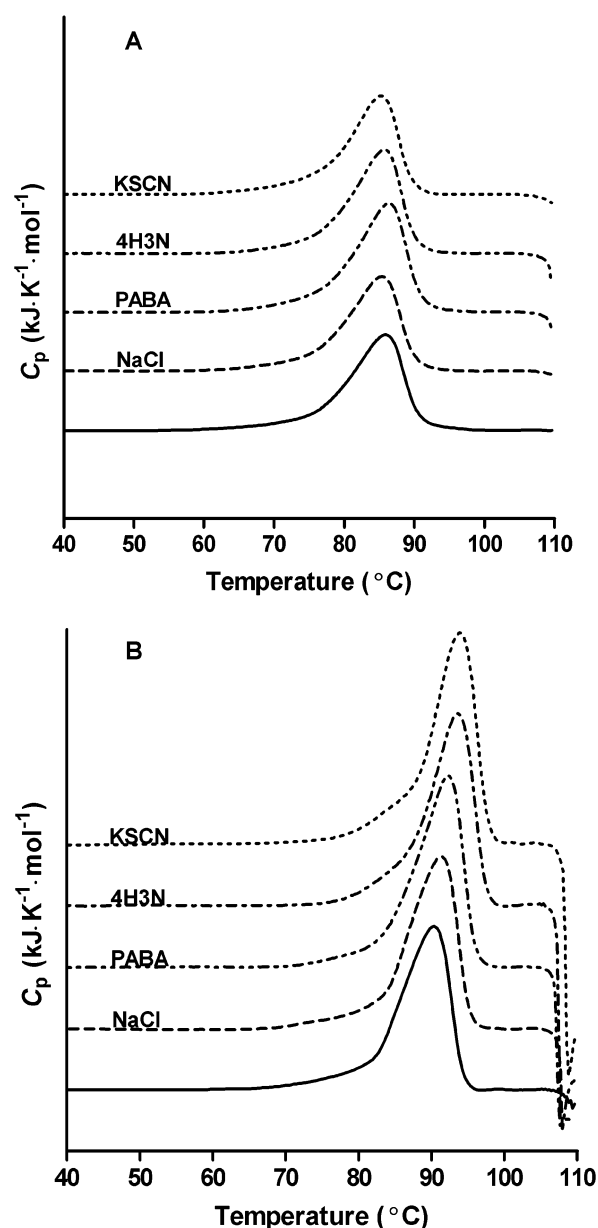


FIGURE 5: DSC thermograms with His^{B10}-site ligands in the absence (A) and presence (B) of 40 mM phenol. Samples contained 0.6 mM human insulin, 0.5 mM Zn^{2+} , and 7 mM phosphate buffer at pH 7.4. Full line, no His^{B10}-site ligand; dashed line, 10 mM NaCl; dash-dot-dot line, 10 mM PABA; dash-dot line, 10 mM 4H3N; and dotted line, 10 mM KSCN.

thermostability of human insulin was studied in the absence and presence of phenol. The addition of 10 mM of the ligands showed only minor effect on the denaturation temperature of zinc-insulin in the absence of phenol (see Figure 5A). The presence of PABA increased the T_{\max} slightly (0.4 $^{\circ}\text{C}$), and 4H3N, NaCl, and KSCN decreased the T_{\max} by 0.2, 0.5, and 0.7 $^{\circ}\text{C}$, respectively. Thus, the effect on insulin T_6 -hexamer was small and ambiguous. KSCN was also tested at high concentrations which should induce the T_3R_3 hexamer conformation in the absence of phenolic ligands (data not shown). The highest KSCN concentration applied was 200 mM, and the DSC thermogram was similar to that of zinc-insulin with no additional ligand (i.e., T_6 -state).

In the presence of phenol, addition of the anionic ligands caused significant increases in T_{\max} (see Figure 5B). The increases with 10 mM ligand were 1.0 (NaCl), 2.0 (PABA),

Table 5: Effects of Addition of 10 mM Anionic Ligands to 0.6 mM Zinc–Insulin in the Absence and Presence of 40 mM Phenol^a

ligand	T_{\max} (°C)	
	without phenol	40 mM phenol
No anionic ligand	86.0	90.3
NaCl (10 mM)	85.5	91.3
PABA (10 mM)	86.4	92.3
4H3N (10 mM)	85.8	93.7
KSCN (10 mM)	85.3	93.8

^a The shown results are the T_{\max} values from DSC experiments.

3.4 (4H3N), and 3.5 °C (KSCN) compared to samples without any anionic ligands. A concentration series of DSC experiments were performed with the anionic ligands with concentrations starting at 1 mM, and the concentration of binding sites for the ligands was held constant at 0.1 mM insulin hexamer. The numbers of binding sites per insulin hexamer were close to one for 4H3N and KSCN; for NaCl and PABA, they were 0.51 and 0.64, respectively. A van't Hoff plot of the logarithms of the ligand concentrations as a function of $1/T_{\max}$ is shown in Figure 6. The results of fitting of the data to eq 3 is given in Table 6 together with the results of $\Delta H_{\text{vH,cal}}$ and ΔH_{cal} and the ratios between these two enthalpies. All four anionic ligands exhibit linear relationship in the van't Hoff plots. The values of $\Delta H_{\text{vH,s}}$ were significantly different for NaCl and PABA compared to those obtained with 4H3N and KSCN and with the different phenolic ligands. Dissociation constants of binding of the four anionic ligands to zinc–insulin saturated with phenol were calculated according to the procedure described above for the phenolic ligands. On the basis of the analysis of number of binding sites (see Table 4), it was assumed that one anionic ligand binds per hexamer, although, apparently, the binding of NaCl and PABA was too weak to saturate the binding site. The apparent dissociation constants, $K_{\text{D},90^\circ\text{C}}$, were 117 (NaCl), 12 (PABA), 1.7 (4H3N), and 1.5 mM (KSCN). The difference between the dissociation constants of 4H3N and KSCN was not significant. In addition, the binding of KSCN was investigated in the presence of resorcinol. In this case, the number of binding sites for KSCN was found to be close to 2, and the binding affinity was 0.45 mM. The enthalpy of denaturation, ΔH_{cal} , was comparable for NaCl, PABA, and 4H3N (from 231 to 243 kJ/mol) and slightly higher for KSCN at 258 kJ/mol. The calorimetric van't Hoff enthalpy, $\Delta H_{\text{vH,cal}}$, was also similar for all four anionic ligands. The ratio $\Delta H_{\text{vH,cal}}/\Delta H_{\text{cal}}$

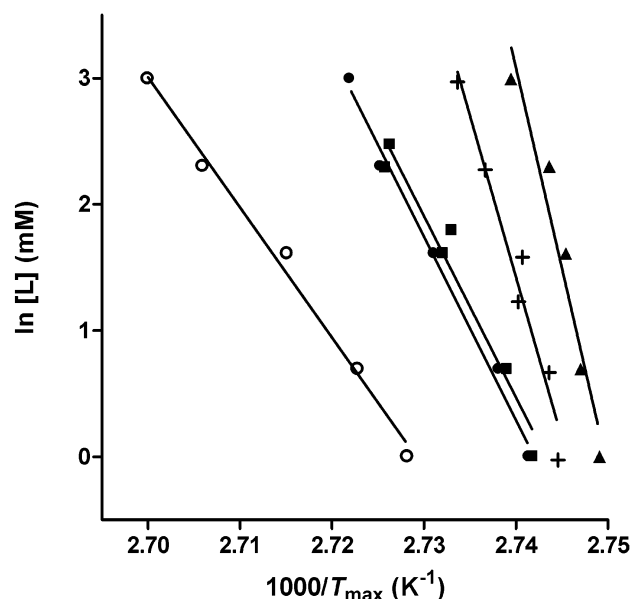


FIGURE 6: van't Hoff plot according to eq 3. The logarithms of the ligand concentrations (mM) are plotted as a function of $1/T_{\max}$ (K^{-1}). Samples contained 0.6 mM human insulin, 0.5 mM Zn^{2+} , 40 mM phenol (or, for KSCN, resorcinol), and 7 mM phosphate at pH 7.4. Ligand legends: 4H3N (squares), KSCN with phenol (full circles), KSCN with resorcinol (open circles), PABA (crosses), and NaCl (triangles). The straight lines are the best fit of the data to eq 3.

was similar for NaCl, PABA, and 4H3N averaging at 6.6 but slightly smaller for KSCN with a ratio of 6.0.

DISCUSSION

Interaction of Phenolic Ligands with Zinc-Free Insulin. Preservative agents such as phenol, *m*-cresol, and benzyl alcohol have been found to destabilize proteins in liquid formulations in numerous studies. Some studies evaluated the effect of preservative agents by DSC experiments, and all found a decrease in the T_{\max} of the thermal denaturation (33–36). It is therefore not surprising that phenol, *m*-cresol, and resorcinol cause a decrease in T_{\max} for the dimeric zinc-free insulin which has no specific binding sites for the phenolic ligands in its native state. The decrease was comparable for all three compounds (0.9–1.4 °C) when used at 20 mM. At 100 mM, the destabilizing effect was obviously much larger with *m*-cresol than with phenol or resorcinol. The exact mechanism of protein destabilization by phenolic preservative agents is not known. However, it is generally believed that the phenolic compounds exert hydrophobic

Table 6: Thermodynamic Parameters Obtained from Analysis of the DSC Experiments with Anionic Ligands and Zinc–Insulin in the Presence of 40 mM Phenol and for KSCN Also in the Presence of 40 mM Resorcinol^a

anionic ligand	ΔH_{cal} (kJ/mol) ^b	$\Delta H_{\text{vH,cal}}$ (kJ/mol) ^c	$\Delta H_{\text{vH,cal}}/\Delta H_{\text{cal}}$	$\Delta H_{\text{vH,s}}$ (kJ/mol) ^d	Goodness of fit (r^2) ^d	$K_{\text{D},90^\circ\text{C}}$ (mM) ^e
No anionic ligand	229 ± 9	1597 ± 29	6.9 ± 0.1	-	-	-
NaCl	231 ± 6	1559 ± 27	6.8 ± 0.2	443 ± 62	0.944	117
PABA	243 ± 7	1590 ± 35	6.5 ± 0.3	354 ± 37	0.958	12
4H3N	241 ± 11	1593 ± 55	6.6 ± 0.4	199 ± 21	0.956	1.7
KSCN	258 ± 14	1546 ± 56	6.0 ± 0.1	201 ± 11	0.991	1.5
KSCN (with resorcinol)	288 ± 8	2012 ± 66	7.0 ± 0.3	286 ± 15	0.992	0.45

^a The enthalpies are the average of the results performed with varying concentrations of each ligand. The enthalpies are given per monomer of insulin ± standard deviation. ^b Area under the curve of the individual excess heat capacity curve. ^c Calculated by eq 7. ^d Best linear least-squares fit of the $\ln[L]$ versus $1/T_{\max}$ data according to eq 3 assuming 1 anionic binding site per insulin hexamer (T_3R_3). ^e Calculated according to eqs 5 and 6. Values are estimated to be in error by no more than 14%.

interactions with hydrophobic patches of the protein. The hydrophobic patches of the protein become exposed upon unfolding, and the phenolic compounds therefore favor the unfolded or partially unfolded state of the protein, consequently causing destabilization. The hydrophobicity of *m*-cresol is the largest of the three phenolic ligands, and this may explain the increased destabilization effect of *m*-cresol. The exotherm following or overlapping the unfolding endotherm in the presence of 100 mM *m*-cresol is probably an aggregation process, which is accelerated by *m*-cresol binding to aggregation-prone unfolded or partially unfolded species. Studies with other proteins have also shown a larger destabilizing effect of *m*-cresol compared to phenol and resorcinol (33, 35).

Thermostability of the Insulin Hexamer Conformations. The binding of phenolic ligands stabilizes the conformation states to T_3R_3 and R_6 relative to T_6 . The phenolic ligand binding was shown to increase the thermodynamic stability of hexameric insulin resulting in a large increase in T_{\max} which is driven by similar relative changes in enthalpy and entropy. The increased stability is caused by the specific binding of the phenolic ligands, which further induces the formation of helical structure in residues 1–8 in the insulin B-chain. The binding of phenol has been found to include two hydrogen bonds from the OH group of phenol to the carbonyl oxygen and amide nitrogen of the A6 and A11 cysteines of insulin. Furthermore, the aromatic ring structure of phenol makes van der Waals contacts with the His^{B5} in the adjacent dimer (9). In this way, phenol stabilizes the hexamer by increasing the interaction in the dimer–dimer interfaces. Resorcinol and *m*-cresol have been reported to form the same interactions in the insulin hexamer as phenol. Additionally, it was shown that the second hydroxyl group of resorcinol forms a second hydrogen bond with the carbonyl oxygen of A11^{Cys} via a water molecule (37). The extra hydrogen bond of resorcinol is responsible for a larger intrinsic heat of binding compared to phenol and *m*-cresol in ITC experiments (22). This may account for the increased enthalpy of thermal denaturation (ΔH_{cal}) for resorcinol compared to phenol and *m*-cresol as found in the present DSC studies. However, the increased enthalpy with resorcinol may also be explained by the 3 apparent additional binding sites occupied by resorcinol compared to phenol and *m*-cresol.

Because of the specific binding of phenolic ligands in the zinc–insulin T_3R_3 and R_6 hexamer, it was expected that these ligands would increase the thermostability of zinc–insulin. All three ligands (phenol, *m*-cresol, and resorcinol) clearly increased the T_{\max} of thermal denaturation in a concentration dependent manner as shown for phenol in Figure 3. With the exception of *m*-cresol, which reaches a plateau (discussed below), the transition temperature did not reach a maximum but kept rising with increasing phenolic ligand concentration. At the high ligand concentrations applied here, it is expected that all binding sites are occupied so the increase in T_{\max} is not caused by increases in occupation of the binding sites, and it is therefore not a manifestation of increased thermodynamic stability of the hexamer itself. It can be predicted from eq 3 that T_{\max} does not reach a maximum (29) and our data correlate well to the equation (see Table 3). Further stabilization of the T_3R_3 or R_6 hexamer with increased concentrations of phenolic ligands did not increase the

enthalpy, but the overall stability was increased which results in increasing T_{\max} , and it must therefore be an entropy-driven stabilization. The increased stability (T_{\max}) can simply be seen as a consequence of the principle of Le Chatelier. An increased ligand concentration will push the equilibrium of eq 2 toward the native protein–ligand complex. This effect is proportional to the ligand affinity and the free ligand concentration. More specifically, the observed Le Chatelier effect is due to the increase in free ligand concentration that decreases the entropy of mixing the dissociated ligand in the medium, and this in turn increases the free energy of the protein–ligand complex (25).

Contrary to the phenol and resorcinol effect on T_{\max} , it was observed that T_{\max} reached a plateau at increasing *m*-cresol concentrations. This phenomenon is probably caused by ligand interaction with both the native and the unfolded state of insulin. As shown with zinc-free insulin, *m*-cresol caused the largest destabilization presumably due to interaction with the unfolded state of insulin. The plateau value depends on the relative affinities of the ligand to the folded and unfolded protein (25). The affinity of *m*-cresol to unfolded insulin is the largest of the phenolic ligands, and at high concentrations, the effect on the unfolded state counteracts the stabilizing effect on the native hexamer and a plateau is observed. The affinities of phenol and resorcinol for the unfolded state relative to the native state are not sufficient to reach a plateau in T_{\max} within the applied concentration range.

Phenolic Ligand Binding Stoichiometry and Affinity. The results of the spectroscopic titrations with phenolic ligands showed that saturation of the anionic sites is necessary for *m*-cresol to induce an amount of R-state comparable to the amount induced by phenol and resorcinol. The present results with Zn–insulin agree with studies performed with Co(II)–insulin (12). However, the results of the present DSC studies showed that both phenol and *m*-cresol bind in only three sites of the insulin hexamer, both in the absence and presence of 50 mM NaCl. Resorcinol was found to bind in 6 sites in the insulin hexamer. Apparently, the DSC studies show that only resorcinol is able to stabilize the R_6 -state, whereas phenol and *m*-cresol can only stabilize the T_3R_3 -state of the insulin zinc–hexamer at the ligand concentrations applied here (higher concentrations destabilize the protein). The difference between the current DSC studies and all other binding studies with insulin hexamer ligands is the temperature. Whereas most other studies have investigated the binding properties around room temperature, the results obtained by DSC are at the denaturation transition temperature, which is 85–95 °C depending on the ligands applied. It has been shown that there is inter-trimer negative cooperativity in the binding of phenolic ligands in the hexamer, and the affinity for the first three phenolic molecules is larger than the affinity for the last three molecules in the R_6 hexamer (16, 22, 38–39). Also, it has been shown that the binding affinities of the three phenolic ligands decrease with increasing temperature (22). In conclusion, we propose that the binding affinity of phenol and *m*-cresol to the second trimer (i.e., to give the R_6 conformation state) is so weak that at the high temperatures of unfolding they have dissociated from the R_6 -state and it is actually the T_3R_3 -state that is present. On the other hand, the binding of resorcinol is strong enough to retain the R_6 -state throughout the thermal

unfolding. This theory is supported by the results of the binding stoichiometry of the anionic ligands. It was shown that in the presence of phenol, the number of binding sites for thiocyanate was approximately 1 and in the presence of resorcinol, the number of binding sites was approximately 2. This is in excellent agreement with the assumption of T_3R_3 -state with phenol and R_6 -state with resorcinol, since one thiocyanate binds to each R_3 trimer unit. This also explains why the difference between phenol and *m*-cresol observed at room temperature in spectroscopic titrations at low anionic ligand concentration is not observed in the DSC results. At room temperature, *m*-cresol was found to only partly drive the T to R transition, whereas phenol fully stabilizes the R_6 -state. Thus, in the DSC studies, where they presumably both stabilize the T_3R_3 -state, no difference is observed between phenol and *m*-cresol.

It was found that the binding affinity of phenol and *m*-cresol were similar and only slightly different from resorcinol. However, since phenol and *m*-cresol apparently stabilize the T_3R_3 -state, they cannot be compared with resorcinol, which stabilizes the R_6 -state since the thermodynamic stabilities of the two states cannot be assumed to be similar. Also, the affinity determined for resorcinol represents an average of all 6 binding sites, whereas the affinity for phenol and *m*-cresol represents only the first 3 binding sites. Since the binding of the last three ligands is much weaker than the first three, the resorcinol affinity will be underestimated in comparison with phenol and resorcinol. Therefore, the apparent binding affinities of phenol and *m*-cresol cannot be compared to the affinities of resorcinol in the present study.

Birnbaum et al. (22) studied the same three ligands by ITC and determined the intrinsic binding constant (K_0) for each ligand in the presence of 50 mM NaCl. The relative K_0 values of the three ligands were 8780, 5040, and 3370 M^{-1} for resorcinol, phenol, and *m*-cresol, respectively. Birnbaum et al. (22) also report the intrinsic heats of binding (enthalpy change) and found that the value is greater for resorcinol than for phenol and *m*-cresol, which is explained by the additional hydrogen bond formed between resorcinol and insulin. The overall free energy of binding was identical for phenol and *m*-cresol and larger for resorcinol. The authors conclude that the order of binding affinity is resorcinol \gg phenol \geq *m*-cresol (22). In the present study, we found comparable enthalpies for the dissociation/unfolding of the protein–ligand complex for phenol and *m*-cresol and higher enthalpy for resorcinol. Thus, qualitatively, the results correlate well between ITC and DSC, but the DSC does not give the intrinsic binding constant. The same order of phenolic ligand affinity to the insulin hexamer has been found by several spectroscopic methods. The effectiveness of driving the T_6 to R_6 conversion of cobalt–insulin hexamer in the absence and presence of NaCl has been found to be resorcinol $>$ phenol $>$ *m*-cresol (12). As observed in the present study with zinc–insulin, the ability of *m*-cresol to stabilize R-state of cobalt–insulin was much weaker in the absence of anionic ligand (12). In another study with cobalt–insulin, the order of affinity was found to be resorcinol $>$ *m*-cresol $>$ phenol, but the content of anionic ligand was not described (40). The stability of insulin zinc–hexamers against extraction of zinc with the reagent 2,2',2''-terpyridine was found to be significantly greater with resorcinol than

with phenol (17). When the spectral changes of the PABA–cobalt–insulin complex were used, it was also found that resorcinol is a stronger ligand than phenol (39). Modeling of circular dichroism spectroscopic titrations of zinc– and cobalt–insulin with phenol and *m*-cresol gave slightly different results with cobalt–insulin, but with zinc–insulin, there was no difference between phenol and *m*-cresol. These studies were performed in the presence of 25 mM chloride (41). The influence of phenolic ligand affinity is also thought to correlate with their effect on chemical stability. It has been found that phenol stabilized insulin formulations against deamidation and polymerization far better than *m*-cresol both in the absence and presence of chloride (10). Thus, results in the literature show that resorcinol binds significantly stronger than phenol and *m*-cresol. The relative effectiveness between phenol and *m*-cresol is ambiguous and dependent on the presence of anionic ligand, but most studies find phenol to be the stronger ligand.

Anionic Ligands. The anionic His^{B10}-zinc anion binding site is formed upon conversion to the T_3R_3 or R_6 insulin hexamer. In the absence of phenolic ligands, zinc–insulin is normally in the T_6 conformation. As shown in Figure 5 and Table 5, the effect of 10 mM of the four tested anionic ligands on zinc–insulin in the absence of phenolic ligand was small and varied. Only one of the anionic ligands (PABA) caused a slight increase in T_{max} , and the three other ligands (NaCl, KSCN, and 4H3N) reduced T_{max} slightly. In contrast, in the presence of phenol, the same concentration of the anionic ligands caused significant increases in T_{max} . The anionic ligands do not change the conformation of the hexamer, but the binding in the His^{B10}-zinc-site stabilizes the T_3R_3 or R_6 hexamer conformation. X-ray (42) and NMR (43) studies have shown that the anions coordinate to the zinc ions and form van der Waals contacts with the Leu^{B6} methyl groups. Addition of the PABA, 4H3N, and KSCN in the presence of phenol caused slight increases in ΔH_{cal} compared to samples containing only phenol. The only significant increase was caused by KSCN, which increased ΔH_{cal} from 229 to 258 kJ/mol. This indicates that the coordination of KSCN in the hexamer is more favorable in terms of enthalpic factors than the coordination of the three other ligands. KSCN also had the highest binding affinity followed by 4H3N, PABA, and NaCl, respectively.

The increases in T_{max} caused by the anionic ligands were found to be concentration-dependent and followed the mechanism described in eq 3 yielding linear van't Hoff plots (Figure 6) analogous to the mechanism described for the phenolic ligands. The relative affinities to cobalt– and zinc–insulin hexamers of a considerable number of anionic ligands have been published by Huang et al. (19), who used 4H3N as a spectroscopic probe in displacement studies in the presence of phenol. There is a good correlation between the results obtained in the present study and the results obtained with zinc–insulin in the 4H3N displacement studies (19). The same study found a significant metal ion effect on the binding of the inorganic anions chloride and thiocyanate to zinc– or cobalt–insulin (19). This finding emphasizes the value of a calorimetric method where zinc–insulin can be studied directly. However, for accurate determinations of the binding affinity, it is important that the binding site is saturated in the DSC experiments. The binding of NaCl and PABA was too weak to saturate the binding site. In the data

treatment, it was assumed that these ligands fully occupied one binding site, although only about half of the sites were saturated. This also explains the large difference between the model-dependent $\Delta H_{\text{vH},s}$ for NaCl and PABA and all other values of $\Delta H_{\text{vH},s}$. To fully saturate the binding sites with NaCl and PABA, much higher concentrations would be necessary; however, this was not possible due to limited solubility of PABA and insulin precipitation (during the DSC scan) in the presence of higher NaCl concentrations.

The existence of T_3R_3 in insulin crystals has been demonstrated by X-ray crystallography (9, 44–45). In the absence of phenolic ligands, T_3R_3 crystals can be obtained in the presence of thiocyanate (42). The existence of a thiocyanate-induced T_3R_3 -state in solution has been shown in several studies. The conversion to T_3R_3 in solution is induced by 30–50 mM thiocyanate, which corresponds to the concentration required to make T_3R_3 crystals (6, 17, 46–47). In the present study, up to 200 mM KSCN was used in DSC studies with zinc–insulin and no stabilizing effect was observed compared to the T_6 zinc–insulin. Thus, even though it has been shown that the R_3 unit in KSCN-induced T_3R_3 is more stable than the T_3 units in the T_6 hexamer (17), the present results show that apparently the thiocyanate-stabilized T_3R_3 -state does not have a higher thermostability than the T_6 -state, whereas the phenol- and *m*-cresol-stabilized T_3R_3 -state did have a significantly higher thermostability than the T_6 -state. This observation may be explained by a weaker binding of thiocyanate at elevated temperatures and by that fact that it dissociates from the hexamer at temperatures below the thermal denaturation temperature of the T_6 hexamer.

The $\Delta H_{\text{vH},\text{cal}}/\Delta H_{\text{cal}}$ ratio. Theoretically, the $\Delta H_{\text{vH},\text{cal}}/\Delta H_{\text{cal}}$ ratio should equal 6 due to the hexameric coordination of zinc–insulin. However, in numerous experiments, we found ratios significantly higher, with values reaching up to 7.1. The applied equation for calculation of $\Delta H_{\text{vH},\text{cal}}$ presumes equilibrium denaturation, but the thermal denaturation of zinc–insulin is only about 80% reversible (28). According to Privalov and Potekhin (31), if the unfolding of the protein is followed by an irreversible denaturation step, then there is no longer full equilibrium between folded and unfolded protein, since the concentration of the unfolded state decreases. A decrease in concentration of unfolded protein will render the unfolding transition narrower, which means that $\Delta H_{\text{vH},\text{cal}}$, and consequently $\Delta H_{\text{vH},\text{cal}}/\Delta H_{\text{cal}}$, becomes larger (31). Another explanation could be that some hexamers associate to form larger, soluble aggregates. Solution studies have shown that this may be the case with zinc–insulin at pH 7.3 (48) and pH 8.0 (49). If these larger aggregates are present in the current study, they could increase the $\Delta H_{\text{vH},\text{cal}}/\Delta H_{\text{cal}}$ ratio in the DSC experiments. KSCN was found to give a lower ratio than the other anionic ligands. The ratio did not vary with the KSCN concentration, so apparently only 1 mM KSCN was needed to reduce the ratio. In contrast, it was found that the ratio of $\Delta H_{\text{vH},\text{cal}}/\Delta H_{\text{cal}}$ increased with increasing resorcinol concentrations (data not shown). It is therefore possible that resorcinol either accelerates an irreversible denaturation step or increases the stability of larger aggregates and that thiocyanate exerts an effect in the opposite direction. On the basis of the present results, it is not possible to draw conclusions about the origin of the increased $\Delta H_{\text{vH},\text{cal}}/\Delta H_{\text{cal}}$ ratios.

In conclusion, we have found that the increase in hexameric insulin thermostability is clearly correlated to the binding of phenolic ligands and the allosteric state of the hexamer, the ligand-stabilized R_6 hexamer being considerably more thermostable than the ligand-stabilized T_3R_3 hexamer, which in turn is more stable than the T_6 hexamer. Differential scanning calorimetry can be used to determine the relative affinities of phenolic and anionic ligands without the use of chromophoric probes or substitution of zinc with cobalt, provided that the binding is strong enough to saturate the sites at temperatures up to the unfolding transition. It is not possible to conclude from the DSC results alone what the allosteric state of the hexamer is. Apparently, the binding of phenol and *m*-cresol is not strong enough to maintain the R_6 -state up to the unfolding temperature, and the insulin hexamer unfolds from the T_3R_3 -state. Similarly, the binding of thiocyanate, in the absence of phenolic ligand, is not strong enough to maintain the T_3R_3 -state up to the unfolding temperature, and the insulin hexamer unfolds from the T_6 -state.

ACKNOWLEDGMENT

The authors thank Niels C. Kaarsholm at Novo Nordisk A/S for valuable discussions.

REFERENCES

1. Blundell, T. L. (1972) Three-dimensional atomic structure of insulin and its relationship to activity, *Diabetes* 21, 492–505.
2. Grant, P. T., Coombs, T. L., and Frank, B. H. (1972) Differences in the nature of the interaction of insulin and proinsulin with zinc, *Biochem. J.* 126, 433–440.
3. Goldman, J., and Carpenter, F. H. (1974) Zinc binding, circular dichroism, and equilibrium sedimentation studies on insulin (bovine) and several of its derivatives, *Biochemistry* 13, 4566–4574.
4. Summerell, J. M., Osmand, A., and Smith, G. H. (1965) An equilibrium-dialysis study of binding of zinc to insulin, *Biochem. J.* 95, 31.
5. Emdin, S. O., Dodson, G. G., Cutfield, J. M., and Cutfield, S. M. (1980) Role of zinc in insulin biosynthesis. Some possible zinc–insulin interactions in the pancreatic B-cell, *Diabetologia* 19, 174–182.
6. Kaarsholm, N. C., Ko, H. C., and Dunn, M. F. (1989) Comparison of solution structural flexibility and zinc binding domains for insulin, proinsulin, and miniproinsulin, *Biochemistry* 28, 4427–4435.
7. Brader, M. L., Kaarsholm, N. C., Lee, R. W., and Dunn, M. F. (1991) Characterization of the R-state insulin hexamer and its derivatives. The hexamer is stabilized by heterotropic ligand binding interactions, *Biochemistry* 30, 6636–6645.
8. Dunn, M. F. (2005) Zinc–ligand interactions modulate assembly and stability of the insulin hexamer—a review, *BioMetals* 18, 295–303.
9. Derewenda, U., Derewenda, Z., Dodson, E. J., Dodson, G. G., Reynolds, C. D., Smith, G. D., Sparks, C., and Swenson, D. (1989) Phenol stabilizes more helix in a new symmetrical zinc insulin hexamer, *Nature* 338, 594–596.
10. Brange, J., and Langkjaer, L. (1992) Chemical stability of insulin. 3. Influence of excipients, formulation, and pH, *Acta Pharm. Nord.* 4, 149–158.
11. Roy, M., Brader, M. L., Lee, R. W., Kaarsholm, N. C., Hansen, J. F., and Dunn, M. F. (1989) Spectroscopic signatures of the T to R conformational transition in the insulin hexamer, *J. Biol. Chem.* 264, 19081–19085.
12. Choi, W. E., Brader, M. L., Aguilar, V., Kaarsholm, N. C., and Dunn, M. F. (1993) The allosteric transition of the insulin hexamer is modulated by homotropic and heterotropic interactions, *Biochemistry* 32, 11638–11645.
13. Dunn, M. F., Pattison, S. E., Storm, M. C., and Quiel, E. (1980) Comparison of the zinc binding domains in the 7S nerve growth factor and the zinc–insulin hexamer, *Biochemistry* 19, 718–725.

14. Storm, M. C., and Dunn, M. F. (1985) The Glu(B13) carboxylates of the insulin hexamer form a cage for Cd^{2+} and Ca^{2+} ions, *Biochemistry* 24, 1749–1756.
15. Kaarsholm, N. C., and Dunn, M. F. (1987) Effects of calcium ion on ternary complexes formed between 4-(2-pyridylazo)-resorcinol and the two-zinc insulin hexamer, *Biochemistry* 26, 883–890.
16. Birnbaum, D. T., Kilcomons, M. A., DeFelippis, M. R., and Beals, J. M. (1997) Assembly and dissociation of human insulin and LysB28ProB29-insulin hexamers: comparison study, *Pharm. Res.* 14, 25–36.
17. Rahuel-Clermont, S., French, C. A., Chou, C. I., Kaarsholm, N. C., and Dunn, M. F. (1997) Mechanisms of stabilization of the insulin hexamer through allosteric ligand interactions, *Biochemistry* 36, 5837–5845.
18. Bloom, C. R., Wu, N., Dunn, A., Kaarsholm, N. C., and Dunn, M. F. (1998) Comparison of the allosteric properties of the Co(II)- and Zn(II)-substituted insulin hexamers, *Biochemistry* 37, 10937–10944.
19. Huang, S. T., Choi, W. E., Bloom, C., Leuenberger, M., and Dunn, M. F. (1997) Carboxylate ions are strong allosteric ligands for the HisB10 sites of the R-state insulin hexamer, *Biochemistry* 36, 9878–9888.
20. Brader, M. L. (1997) Zinc coordination, asymmetry, and allostery of the human insulin hexamer, *J. Am. Chem. Soc.* 119, 7603–7604.
21. Bonaccio, M., Ghaderi, N., Borchardt, D., and Dunn, M. F. (2005) Insulin allosteric behavior: Detection, identification, and quantification of allosteric states via ^{19}F NMR, *Biochemistry* 44, 7656–7668.
22. Birnbaum, D. T., Dodd, S. W., Saxberg, B. E., Varshavsky, A. D., and Beals, J. M. (1996) Hierarchical modeling of phenolic ligand binding to 2Zn -insulin hexamers, *Biochemistry* 35, 5366–5378.
23. McGraw, S. E., Craik, D. J., and Lindenbaum, S. (1990) Testing of insulin hexamer-stabilizing ligands using theoretical binding, microcalorimetry, and nuclear magnetic resonance (NMR) line broadening techniques, *Pharm. Res.* 7, 600–605.
24. McGraw, S. E., and Lindenbaum, S. (1990) The use of microcalorimetry to measure thermodynamic parameters of the binding of ligands to insulin, *Pharm. Res.* 7, 606–611.
25. Cooper, A., Nutley, M. A., and Wadood, A. (2001) Differential scanning microcalorimetry, in *Protein-Ligand Interactions: Hydrodynamics and Calorimetry* (Harding, S. E., and Chowdry, B. Z., Eds.) 1st ed., pp 287–318, Oxford University Press, Oxford, U.K.
26. Brange, J., Ribel, U., Hansen, J. F., Dodson, G., Hansen, M. T., Havelund, S., Melberg, S. G., Norris, F., Norris, K., Snel, L., Sørensen, A. R., and Voigt, H. O. (1988) Monomeric insulins obtained by protein engineering and their medical implications, *Nature* 333, 679–682.
27. Plotnikov, V. V., Brandts, J. M., Lin, L. N., and Brandts, J. F. (1997) A new ultrasensitive scanning calorimeter, *Anal. Biochem.* 250, 237–244.
28. Huus, K., Havelund, S., Olsen, H. B., van de Weert, M., and Frokjaer, S. (2005) Thermal dissociation and unfolding of insulin, *Biochemistry* 44, 11171–11177.
29. Fukada, H., Sturtevant, J. M., and Quioco, F. A. (1983) Thermodynamics of the binding of L-arabinose and of D-galactose to the L-arabinose-binding protein of *Escherichia coli*, *J. Biol. Chem.* 258, 13193–13198.
30. Schellman, J. A. (1975) Macromolecular binding, *Biopolymers* 14, 999–1018.
31. Privalov, P. L., and Potekhin, S. A. (1986) Scanning microcalorimetry in studying temperature-induced changes in proteins, *Methods Enzymol.* 131, 4–51.
32. D'Auria, S., Barone, R., Rossi, M., Nucci, R., Barone, G., Fessas, D., Bertoli, E., and Tanfani, F. (1997) Effects of temperature and SDS on the structure of beta-glycosidase from the thermophilic archaeon *Sulfolobus solfataricus*, *Biochem. J.* 323, 833–840.
33. Maa, Y. F., and Hsu, C. C. (1996) Aggregation of recombinant human growth hormone induced by phenolic compounds, *Int. J. Pharm.* 140, 155–168.
34. Zhang, Y., Roy, S., Jones, L. S., Krishnan, S., Kerwin, B. A., Chang, B. S., Manning, M. C., Randolph, T. W., and Carpenter, J. F. (2004) Mechanism for benzyl alcohol-induced aggregation of recombinant human interleukin-1 receptor antagonist in aqueous solution, *J. Pharm. Sci.* 93, 3076–3089.
35. Remmele, R. L., Jr., Nightlinger, N. S., Srinivasan, S., and Gombotz, W. R. (1997) Interleukin-1 receptor (IL-1R) liquid formulation development using differential scanning calorimetry, *Pharm. Res.* 15, 200–208.
36. Gupta, S., and Kaisheva, E. (2003) Development of a multidose formulation for a humanized monoclonal antibody using experimental design techniques, *AAPS PharmSci* 5, E8-2003.
37. Smith, G. D., Ciszak, E., Magrum, L. A., Pangborn, W. A., and Blessing, R. H. (2000) R6 hexameric insulin complexed with *m*-cresol or resorcinol, *Acta Crystallogr., Sect. D: Biol. Crystallogr.* 56, 1541–1548.
38. Bloom, C. R., Kaarsholm, N. C., Ha, J., and Dunn, M. F. (1997) Half-site reactivity, negative cooperativity, and positive cooperativity: Quantitative considerations of a plausible model, *Biochemistry* 36, 12759–12765.
39. Bloom, C. R., Choi, W. E., Brzovic, P. S., Ha, J. J., Huang, S. T., Kaarsholm, N. C., and Dunn, M. F. (1995) Ligand binding to wild-type and E-B13Q mutant insulins: A three-state allosteric model system showing half-site reactivity, *J. Mol. Biol.* 245, 324–330.
40. Dodson, E. J., Dodson, G. G., Hubbard, R. E., Moody, P. C. E., Turkenburg, J., Whittingham, J., Xiao, B., Brange, J., Kaarsholm, N., and Thøgersen, H. (1993) Insulin assembly—its modification by protein engineering and ligand-binding, *Philos. Trans. R. Soc. London, Ser. A* 345, 153–164.
41. Jacoby, E., Krüger, P., Karatas, Y., and Wollmer, A. (1993) Distinction of structural reorganisation and ligand binding in the T \leftrightarrow R transition of insulin on the basis of allosteric models, *Biol. Chem. Hoppe-Seyler* 374, 877–885.
42. Whittingham, J. L., Chaudhuri, S., Dodson, E. J., Moody, P. C., and Dodson, G. G. (1995) X-ray crystallographic studies on hexameric insulins in the presence of helix-stabilizing agents, thiocyanate, methylparaben, and phenol, *Biochemistry* 34, 15553–15563.
43. Olsen, H. B., Leuenberger-Fisher, M. R., Kadima, W., Borchardt, D., Kaarsholm, N. C., and Dunn, M. F. (2003) Structural signatures of the complex formed between 3-nitro-4-hydroxybenzoate and the Zn(II)-substituted R_6 insulin hexamer, *Protein Sci.* 12, 1902–1913.
44. Smith, G. D., Swenson, D. C., Dodson, E. J., Dodson, G. G., and Reynolds, C. D. (1984) Structural stability in the 4 zinc human insulin hexamer, *Proc. Natl. Acad. Sci. U.S.A.* 81, 7093–7097.
45. Ciszak, E., and Smith, G. D. (1994) Crystallographic evidence for dual coordination around zinc in the T_3R_3 human insulin hexamer, *Biochemistry* 33, 1512–1517.
46. Brzovic, P. S., Choi, W. E., Borchardt, D., Kaarsholm, N. C., and Dunn, M. F. (1994) Structural asymmetry and half-site reactivity in the T to R allosteric transition of the insulin hexamer, *Biochemistry* 33, 13057–13069.
47. Ferrari, D., Diers, J. R., Bocian, D. F., Kaarsholm, N. C., and Dunn, M. F. (2001) Raman signatures of ligand binding and allosteric conformation change in hexameric insulin, *Biopolymers* 62, 249–260.
48. Cunningham, L. M., Fischer, R. L., and Vestling, C. S. (1955) A study of the binding of zinc and cobalt by insulin, *J. Am. Chem. Soc.* 77, 5703–5707.
49. Fredericq, E. (1956) The association of insulin molecular units in aqueous solutions, *Arch. Biochem. Biophys.* 65, 218–228.